Supporting Information for "Constraints on Southern Ocean Shortwave Cloud Feedback from the Hydrological Cycle"

Chuyan Tan[1], Daniel T. McCoy[1], Gregory S. Elsaesser[2,3]

[1]University of Wyoming

[2]Columbia University, Dept. of Appl. Physics and Appl. Mathematics

[3]NASA Goddard Institute for Space Studies (GISS)

Contents of this file

Introduction This document provides figures supporting the analysis in the main text and a table of all the global climate models examined in the main text.

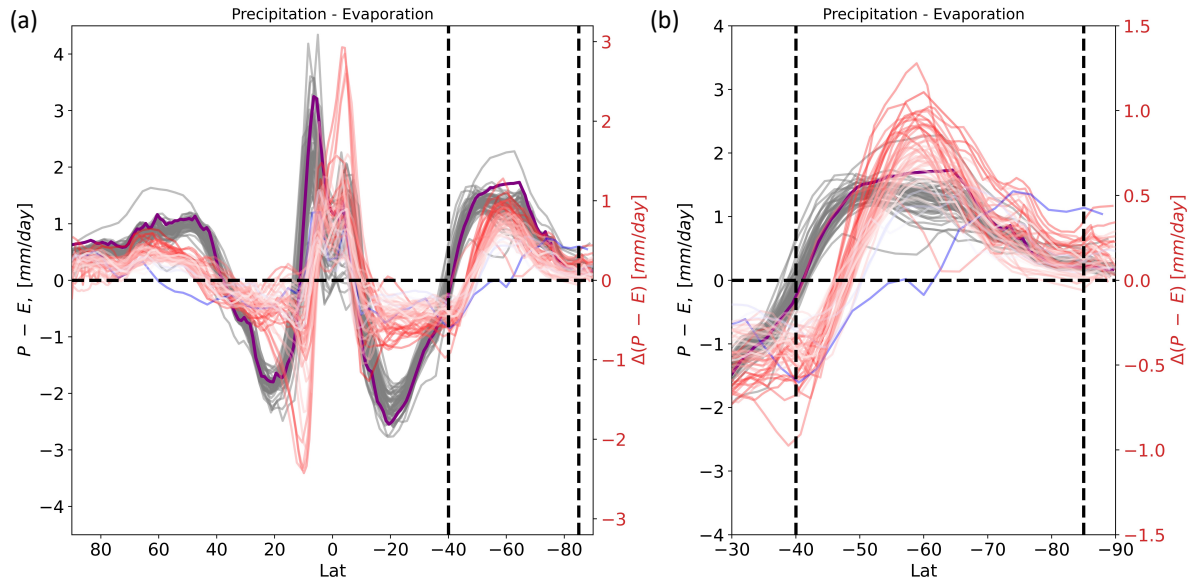

Figure S1. Latitudinal distributions of precipitation minus evaporation ($P - E$) for the globe (a) and the Southern Ocean (b) from GCMs listed in Table S1. The gray lines (left axis) are $P - E$ from the mean-state (*piControl*) simulations. The red and blue lines (right axis) are the changes in $P - E$ ($\Delta P - E$) from the mean-state average to the 140 - 150 years mean of $abrupt4xCO_2$ simulations, colored by $\Delta P - E$ averaged over $40 - 85^oS$. MERRA-2 monthly reanalyses for $P - E$ averaged over $1992 - 2016$ are plotted in thick purple lines for comparison.

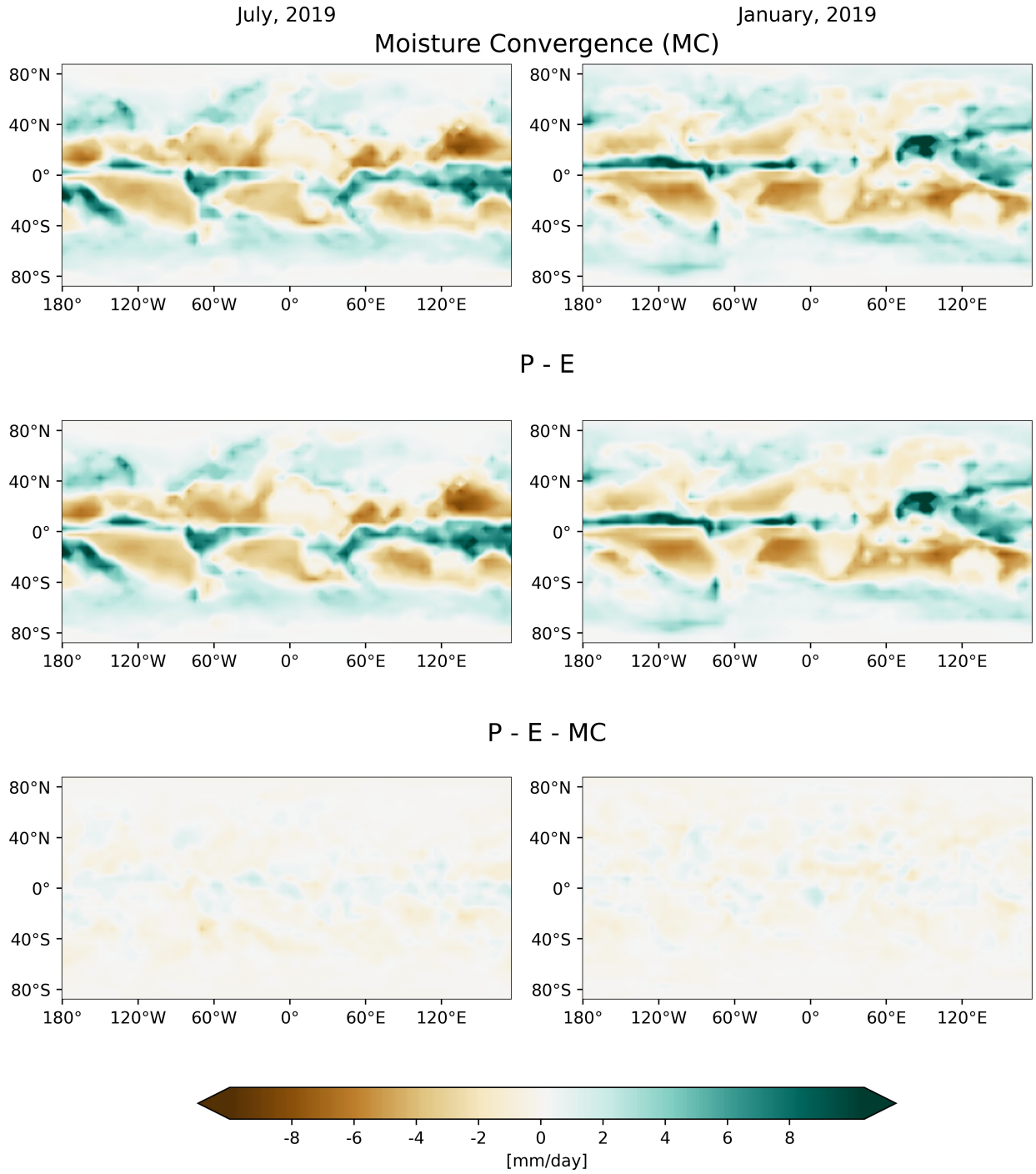

Figure S2. ERA-5 monthly averaged vertical integral of convergence of moisture flux (top), total precipitation - surface evaporation (P - E) (middle), and their difference (bottom). Data are binned into 5^o x 5^o (Lat x Lon) regions. The Pearson correlation coefficient between moisture convergence and $P - E$ in $40 - 85^oS$ region are 0.971 and 0.987 for January and July data, respectively.

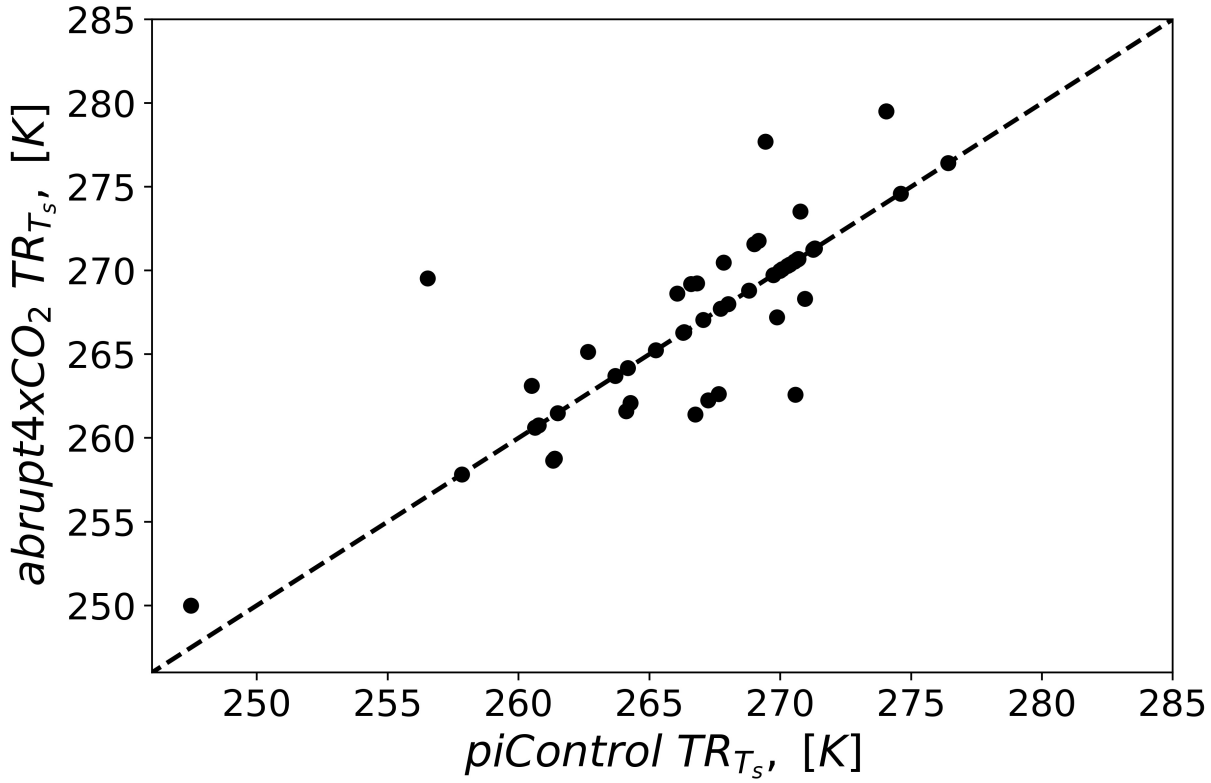

Figure S3. The partition surface skin temperature (TR_{T_s}) of cold and warm regimes from Equation 3 that produce the highest R^2 in predicting $abrupt4xCO_2$ LWP (y-axis) versus predicting *piControl* LWP (x-axis). Dots represent GCMs listed in Table S1. The dashed line is the 1-1 reference line.

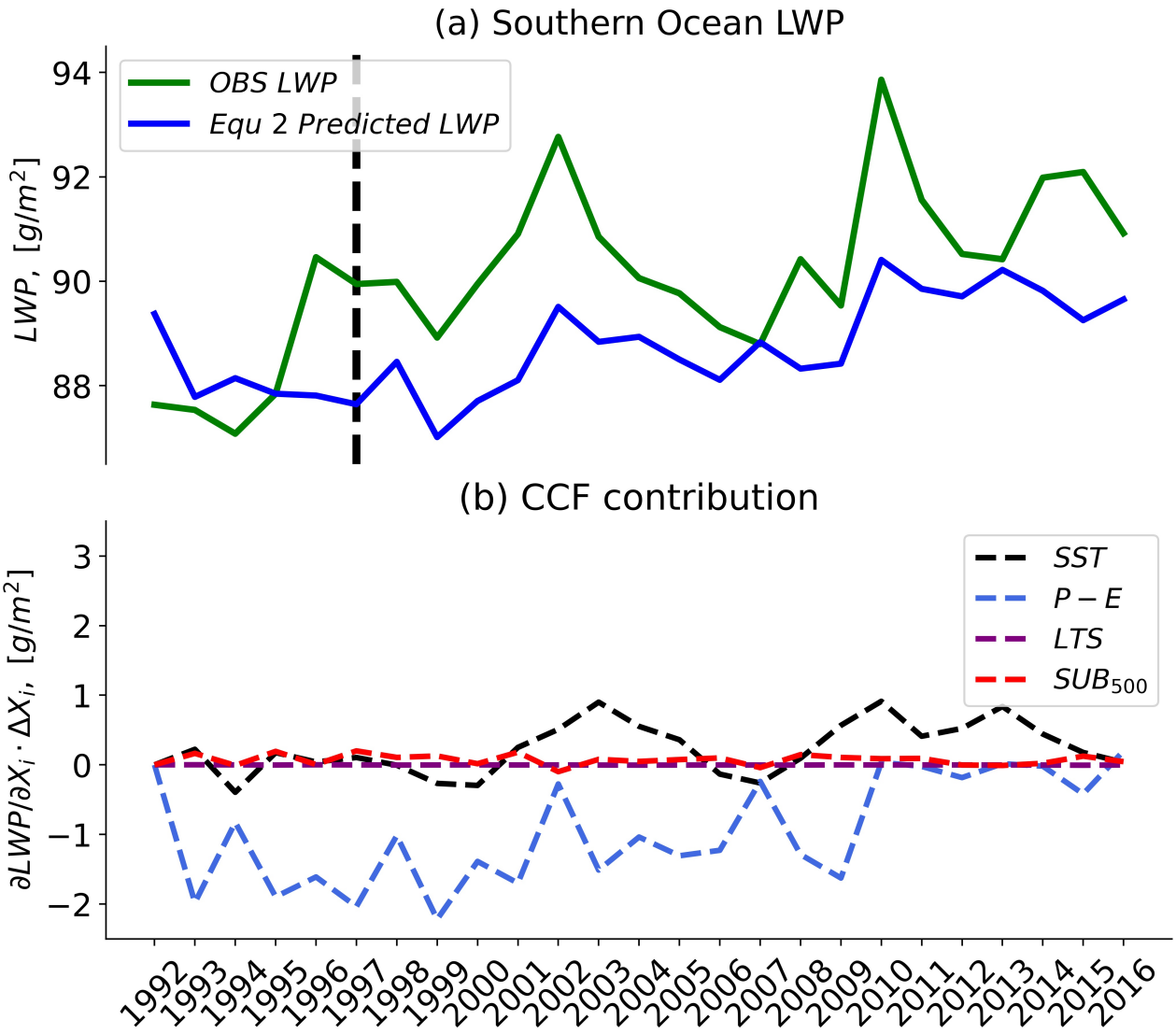

Figure S4. As in Figure 4, except Equation 2 is trained on data from 1992 to 1996 (the left side of the dashed line), and it was used to predict the annual mean LWP from 1997 to 2016. The sensitivity of LWP to CCFs ($\partial LWP/\partial X_i$) is not sensitive to the choice of the training period (comparing the panel b with Fig 4b).

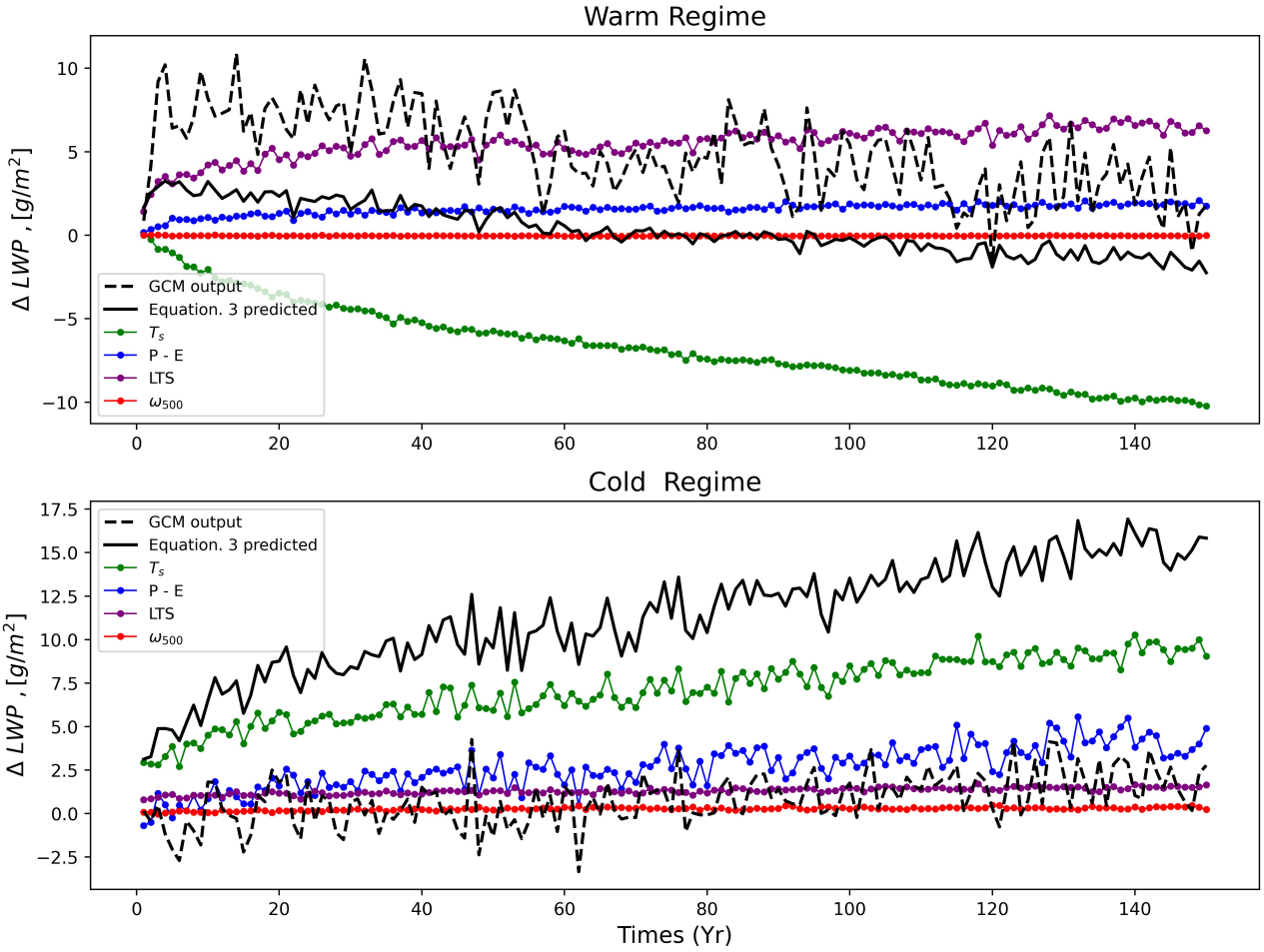

Figure S5. Southern Ocean LWP for 150 years of $abrupt4xCO_2$ simulation of CESM2 compared to the predictions of Equation 3. Time series of the individual CCFs contributions are shown. Cold and warm regime responses are shown separately.

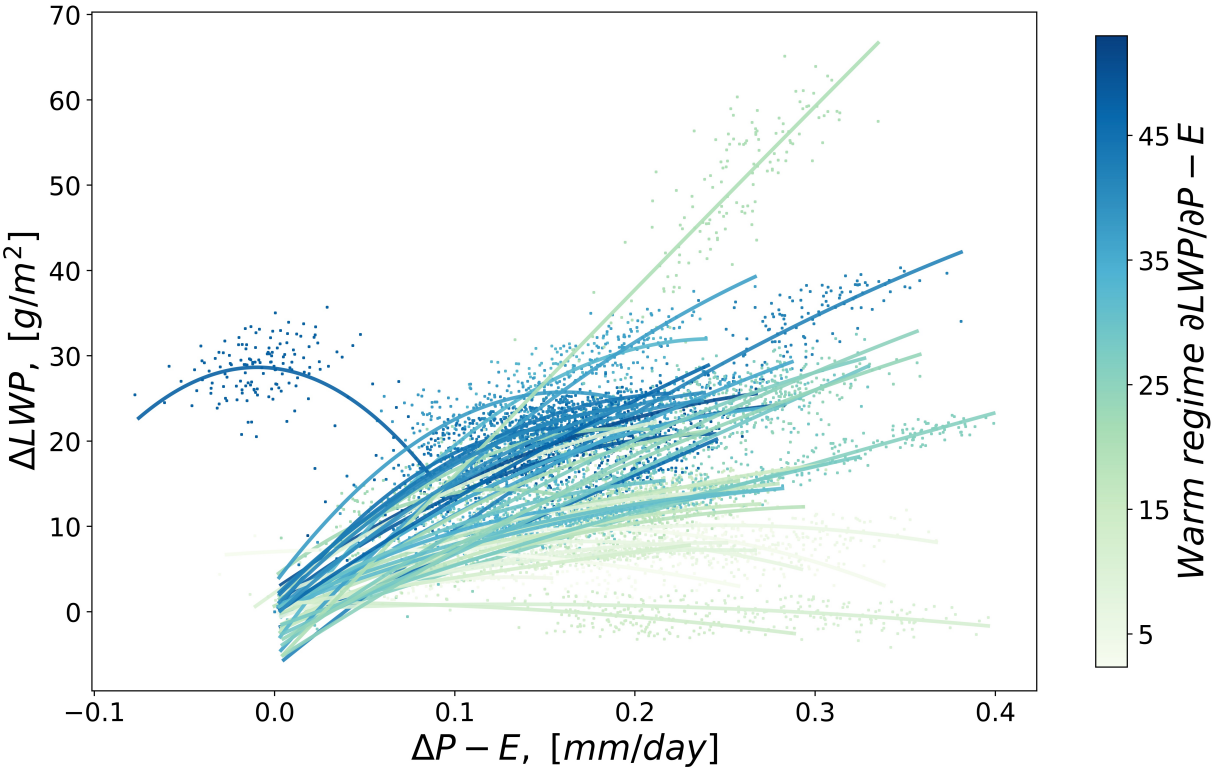

Figure S6. Evolution of LWP versus moisture convergence ($P - E$) averaged over $40 - 85^oS$ in the first 150 years of $abrupt4xCO_2$ simulations. 50 GCMs listed in Table S1 are shown (BNU-ESM is the only GCM predicting reduced $P - E$ in response to global warming). LWP and $P - E$ are shown as anomalies relative to the first-year values of the $abrupt4xCO_2$ simulation. A second-order polynomial function is applied to fit the GCM response. Dots and fitting lines are colored by model warm regime sensitivity of LWP to $P - E$ ($\partial LWP/\partial P - E$) (pink squares in Fig 7). The GCM warm regime $\partial LWP/\partial P - E$ and the LWP response for the entire SO $\Delta LWP/\Delta GMT$ covary across GCMs with a correlation of $r = 0.78$.

Table S1. GCMs used in this study in descending order of effective climate sensitivity (ECS)

Number	Model	CMIP	ECS (K)	Number	Model	CMIP	ECS (K)
1	CanESM5	cmip6	5.64	46	GISS-E2-2-G	cmip6	2.43
2	E3SM-1-0	cmip6	5.31	47	GISS-E2-H	cmip5	2.31
3	CESM-FV2	cmip6	5.16	48	CAMS-CSM1-0	cmip6	2.29
4	CESM2	cmip6	5.15	49	GISS-E2-R	cmip5	2.12
5	CNRM-CM6-1	cmip6	4.90	50	INM-CM4-8	cmip6	1.83
6	CESM2-WACCM-FV2	cmip6	4.80				
7	CNRM-ESM2-1	cmip6	4.79				
8	NESM3	cmip6	4.76				
9	IPSL-CM6A-LR	cmip6	4.70				
10	CESM2-WACCM	cmip6	4.68				
11	MIROC-ESM	cmip5	4.65				
12	TaiESM1	cmip6	4.36				
13	EC-Earth3-Veg	cmip6	4.33				
14	CNRM-CM6-1-HR	cmip6	4.33				
15	EC-Earth3	cmip6	4.26				
16	FGOALS-s2	cmip5	4.18				
17	IPSL-CM5A-LR	cmip5	4.13				
18	CSIRO-Mk3-6-0	cmip5	4.09				
19	BNU-ESM	cmip5	4.04				
20	GFDL-CM3	cmip5	3.95				
21	GFDL-CM4	cmip6	3.89				
22	SAMO-UNICON	cmip6	3.72				
23	CanESM2	cmip5	3.70				
24	MPI-ESM-LR	cmip5	3.63				
25	CMCC-CM2-SR5	cmip6	3.55				
26	MPI-ESM-MR	cmip5	3.45				
27	FGOALS-g2	cmip5	3.37				
28	BCC-ESM1	cmip6	3.25				
29	CNRM-CM5	cmip5	3.25				
30	AWI-CM-1-1-MR	cmip6	3.16				
31	MRI-ESM2-0	cmip6	3.13				
32	GISS-E2-1-H	cmip6	3.12				
33	MPI-ESM1-2-LR	cmip6	3.03				
34	CCSM4	cmip5	2.94				
35	NorESM1-M	cmip5	2.87				
36	FGOALS-g3	cmip6	2.87				
37	bcc-csm1-1	cmip5	2.82				
38	MIROC5	cmip5	2.71				
39	GISS-E2-1-G	cmip6	2.71				
40	MIROC-ES2L	cmip6	2.66				
41	MRI-CGCM3	cmip5	2.61				
42	MIROC6	cmip6	2.60				
43	NorESM2-MM	cmip6	2.49				
44	GFDL-ESM2M	cmip5	2.44				
45	GFDL-ESM2G	cmip5	2.43				